The biter bit? Investigation of possible *in-ovo* self-envenomation in an Egyptian saw-scaled viper using region of interest X-ray microtomography

John Mulley, Richard E Johnston

Proven examples of self-envenomation by venomous snakes, and especially instances of death as a result of these events, are extremely rare, if not non-existent. Here we use Region of Interest X-ray microtomography to investigate a putative case of fatal *in-ovo* self-envenomation in the Egyptian saw-scaled viper, *Echis pyramidum*. Our analyses have provided unprecedented insight into the skeletal anatomy of a late-stage embryonic snake and the disposition of the fangs without disrupting or destroying a unique biological specimen.

PeerJ PrePrints

PeerJ PrePrints | http://dx.doi.org/10.7287/peerj.preprints.624v1 | CC-BY 4.0 Open Access | rec: 19 Nov 2014, publ: 19 Nov 2014

Title page

The biter bit? Investigation of possible *in-ovo* self-envenomation in an Egyptian saw-scaled viper using region of interest X-ray microtomography

Richard E Johnston[1] and John F Mulley[2*]

1. College of Engineering, Swansea University, Swansea, SA2 8PP, United Kingdom

2. School of Biological Sciences, Bangor University, Bangor, Gwynedd LL57 2UW, United Kingdom

*To whom correspondence should be addressed (j.mulley@bangor.ac.uk)

PeerJ PrePrints

Abstract

Proven examples of self-envenomation by venomous snakes, and especially instances of death as a result of these events, are extremely rare, if not non-existent. Here we use Region of Interest X-ray microtomography to investigate a putative case of fatal *in-ovo* self-envenomation in the Egyptian saw-scaled viper, *Echis pyramidum*. Our analyses have provided unprecedented insight into the skeletal anatomy of a late-stage embryonic snake and the disposition of the fangs without disrupting or destroying a unique biological specimen.

Keywords

Snake; saw-scaled viper; self-envenomation; microCT; region of interest; X-ray microtomography

Background

Snake venom is a potent mix of proteins and peptides, honed by millions of years of natural selection for rapid prey immobilisation (Casewell et al. 2013). Safely producing and storing this lethal arsenal within the body prior to its use creates obvious issues, and these have to some extent been overcome in snakes by the evolution of a specialised gland (the venom gland (Jackson, 2003; Weinstein, Smith & Kardong, 2009)) for storing venom and by production of inactive precursor proteins (zymogens) for many venom components (Shimokawa et al. 1996; Portes-Junior et al. 2014). The issue of whether a venomous snake is immune to its own venom is still largely unresolved, although there is some evidence of possible adaptations for resistance to self-envenomation (Denson, 1976; Smith et al, 2000; Takacs, Wilhelmsen & Sorota, 2001; Takacs, Wilhelmsen & Sorota, 2004; Tanaka-Azevedo et al. 2004; Vieira et al. 2008). Investigations of the available literature have failed to identify

PeerJ PrePrints

any definitive examples of self-envenomation by a venomous snake, although such tales are prevalent on the internet, where they seemingly rarely cause death or long-term injury. Following some breeding experiments with Egyptian saw-scaled vipers (*Echis pyramidum*) in summer 2014, we found a single egg failed to hatch from a clutch of thirteen otherwise successful eggs. Examination revealed that the developing embryo had used its eggtooth to create slits in the eggshell (and was therefore within a few days of hatching) and, when opened, the egg contained a dead, almost-fully-developed snake, with some un-absorbed yolk (Figure 1a). A coil of the body was firmly located within the mouth (Figures 1b-1d), suggesting a possible case of *in-ovo* self-envenomation. To definitively prove this however, we needed to determine whether the fangs were penetrating the body cavity, ideally without disturbing the positioning of this unique specimen.

High resolution X-ray microtomography (µCT, microCT) is a non-destructive method for imaging internal structures in three dimensions at micron level spatial resolution based upon the principle that X-ray attenuation is a function of X-ray energy and the density and atomic composition of materials being scanned. The result is a 3D 'tomogram' (Maire & Withers, 2014), generated from hundreds or thousands of individual 2D X-ray projections sampled at the detector while the specimen rotates between the fixed X-ray source and detector. The tomogram consists of a matrix of 3D isotropic voxels, each of which is assigned a grayscale value derived from a linear attenuation coefficient that relates to the density of the scanned materials (Landis & Keane, 2010; Cnudde & Boone, 2013). MicroCT resolution can be of the order of 100 times finer than medical CT scans (Ketcham & Carlson, 2001), enabling 3D imaging and analysis of smaller internal features, although resolution is related to specimen width. Successful filtered back projection reconstruction of the 3D data requires the entire sample width to be encompassed within each 2D projection or 'field of view' at all rotations (Kak & Slaney, 2001) and a typical X-ray detector panel in a laboratory microCT setup has a

PeerJ PrePrints

width of around 1000-4000 pixels. For a detector with a width of 2000 pixels, the pixel size (and ultimately 3D voxel size of the reconstructed tomogram) is therefore *w*/2000, where *w* is the maximum width of the specimen.

Conventional wisdom in microCT reconstruction states that only parts of the object illuminated by X-rays in all 2D projections images will be properly reconstructed i.e. the whole object should lie within the field of view for all rotations during the scan. However, this conventional approach produces scans of larger objects at a lower resolution. Region of Interest (RoI) tomography (Kyrieleis et al. 2011) offers the potential to 'zoom in' to particular areas of large specimens so as to provide higher resolution tomograms of key regions. In this approach, parts of the specimen are within the field of view for some rotations, but then rotate out of the field of view at other rotational angles. We carried out Region of Interest microCT to determine the disposition of the fangs in our specimen and so reveal whether the biter had indeed been bit.

Methods

A clutch of thirteen eggs were laid by a wild-caught Egyptian saw-scaled viper (*E. pyramidum*) on the 4th July 2014 and, following incubation at 27°C, all but one had hatched by 4th September 2014. Upon removal from its egg, the specimen was fixed in 4% paraformaldehyde in phosphate buffered saline (pH7.5) and stored at 4°C. The specimen was imaged using a Leica MSV269 stereoscope and an Apple iPhone 5. To minimise physical disruption during shipping, the specimen was packed in paraformaldehyde-soaked cotton wool in a 100ml container (Gosseline TP51-004).

3D geometric data was collected on a Nikon XT H 225 microfocus X-ray tomography system (Nikon Metrology, Tring, UK) at the College of Engineering, Swansea University, UK. Images were captured with a 1.3 Megapixel Varian Paxscan 2520 amorphous silicon flat

PeerJ PrePrints

panel detector, in reflection mode with a molybdenum target. Scans were performed with 65 kV X-ray tube voltage, a current of 295 µA, with an exposure of 2000 ms, capturing 1 image per rotation step of 0.119°, resulting in 3016 images per scan and a voxel (3D pixel) size of 17.6 µm. The tomograms were reconstructed from the 2D projections using Nikon CTPro version 3.1.3 software (Nikon Metrology, Tring, UK). The commercial software VGStudio Max 2.1.5 (Volume Graphics, Heidelberg, Germany) and the free software Drishti (Limaye, 2012) were used to view the reconstructed data, 2D slices and rendered 3D volumes.

Results and discussion

In order to minimise handling and potential disruption of our specimen, it was decided to conduct scans whilst it was still packed in its 52mm diameter container of cotton wool-soaked preservative (Figure 1). Since scans of the entire specimen and its container would have resulted in a lower overall resolution, with a voxel size of approximately 27µm, we employed RoI tomography to 'zoom in' to the snake, ignoring the surrounding materials, resulting in a field of view of 33.75mm and a voxel size of 17.6µm. These RoI scans have provided astonishing insights into the skeletal anatomy of this specimen and clearly reveal the position and orientation of both fangs (Figures 2a-e). The fangs of vipers such as *E. pyramidum* are located on a hinged maxilla, which allows them to be folded against the roof of the mouth when not in use and to swing forward to an erect position during a strike. Perhaps disappointingly, we find that the fangs of this specimen are in the folded position and are not penetrating the body cavity (Figure 2). It is still possible however that a bite and envenomation did take place, followed by subsequent withdrawal of the fangs, where the cause of death could be either a result of venom or the physical trauma associated with the bite itself, especially if one or both fangs punctured a major organ. Alternatively, it is possible that this animal drowned within its egg, after having non-fatally bitten itself and then

PeerJ PrePrints

being either unable or unwilling to release. Whilst it may be possible that disruption of the specimen may reveal traces of bite marks, we feel that the chances of identifiable marks being found are not high enough to risk the permanent loss of this unique specimen.

Although we were unable to determine the cause of death in this case, we were easily able to identify the location and orientation of the fangs and other skeletal structures in this relatively small specimen. Our approach demonstrates the power and utility of non-destructive X-ray microtomography and Region of Interest scanning to shed light on biological problems, especially those involving rare, delicate, or unique specimens. More generally, this project highlights the importance of, awareness of, and collaboration across academic disciplines, in this case biological sciences and materials sciences.

Conclusions

We have successfully used Region of Interest scanning to determine the position of the fangs in an embryonic snake that seemingly died as a result of a self-inflicted bite. Whether death was a direct result of a bite involving penetration of the fangs (envenomation, organ puncture/failure) or an indirect result of a non-penetrative bite (e.g. drowning) is unclear and so the cause of death of this enigmatic specimen remains a mystery.

Acknowledgements

The authors wish to thanks Rhys Morgan for technical assistance and Twitter for facilitating the initial collaboration.

Funding

PeerJ PrePrints

148 JFM has been generously supported by the Biosciences, Environment and Agriculture
149 Alliance between Aberystwyth and Bangor universities. RJ is supported by the College of
150 Engineering at Swansea University.

151

152 **References**

153

154 Casewell, N. R., Wuster, W., Vonk, F. J., Harrison, R. A., Fry, B. G. 2013 Complex
155 cocktails: the evolutionary novelty of venoms. *Trends in Ecology & Evolution.* 28: 219-229.

156

157 Cnudde, V., Boone, M. N. 2013 High-resolution X-ray computed tomography in geosciences:
158 A review of the current technology and applications. *Earth-Science Reviews* 123: 1-17.

159

160 Denson, K. W. 1976 The clotting of a snake (*Crotalus viridis*) plasma and its interaction with
161 various snake venoms. *Thrombosis and Haemostasis* 35: 314-323.

162

163 Jackson, K. 2003 The evolution of venom-delivery systems in snakes. *Zoological Journal of*
164 *the Linnean Society* 137: 337-354.

165

166 Kak, A. C., Slaney, M. 2001 *Principles of Computerized Tomographic Imaging*: Society for
167 Industrial and Applied Mathematics.

168

169 Ketcham, R. A., Carlson, W. D. 2001 Acquisition, optimization and interpretation of X-ray
170 computed tomographic imagery: applications to the geosciences. *Computers & Geosciences*
171 27: 381-400.

172

PeerJ PrePrints

Kyrieleis, A., Titarenko, V., Ibison, M., Connolley, T., Withers, P. J. 2011 Region-of-interest tomography using filtered backprojection: assessing the practical limits. *Journal of Microscopy* 241: 69-82.

Landis, E. N., Keane, D. T. 2010 X-ray microtomography. *Materials Characterization* 61: 1305-1316.

Limaye, A. 2012 Drishti: a volume exploration and presentation tool. *Proc. SPIE 8506, Developments in X-Ray Tomography VIII, 85060X.* (DOI 10.1117/12.935640).

Maire, E., Withers, P. J. 2014 Quantitative X-ray tomography. *International Materials Reviews.* 59: 1-43.

Portes-Junior, J. A., Yamanouye, N., Carneiro, S. M., Knittel, P. S., Sant'Anna, S. S., Nogueira, F. C., Junqueira, M., Magalhaes, G. S., Domont, G. B., Moura-da-Silva, A. M. 2014 Unraveling the processing and activation of snake venom metalloproteinases. *Journal of Proteome Research* 13: 3338-3348.

Shimokawa, K., Jia, L. G., Wang, X. M., Fox, J. W. 1996 Expression, activation, and processing of the recombinant snake venom metalloproteinase, pro-atrolysin E. *Archives of Biochemistry and Biophysics.* 335: 283-294.

Smith, A., Marshall, L. R., Mirtschin, P. J., Jelinek, G. A. 2000 Neutralisation of the clotting activity of Australian snake venoms by snake plasma. *Toxicon.* 38: 1855-1858.

PeerJ PrePrints

198 Takacs, Z., Wilhelmsen, K. C., Sorota, S. 2001 Snake a-Neurotoxin Binding Site on the
199 Egyptian Cobra (*Naja haje*) Nicotinic Acetylcholine Receptor Is Conserved. *Molecular*
200 *Biology and Evolution.* 18: 1800-1809.
201
202 Takacs, Z., Wilhelmsen, K., Sorota, S. 2004 Cobra (Naja spp.) Nicotinic Acetylcholine
203 Receptor Exhibits Resistance to Erabu Sea Snake (*Laticauda semifasciata*) Short-Chain A-
204 Neurotoxin. *Journal of Molecular Evolution* 58: 516-526.
205
206 Tanaka-Azevedo, A. M., Torquato, R. J. S., Tanaka, A. S., Sano-Martins, I. S. 2004
207 Characterization of *Bothrops jararaca* coagulation inhibitor (BjI) and presence of similar
208 protein in plasma of other animals. *Toxicon.* 44: 289-294.
209
210 Vieira, C. O., Tanaka, A. S., Sano-Martins, I. S., Morais, K. B., Santoro, M. L., Tanaka-
211 Azevedo, A. M. 2008 *Bothrops jararaca* fibrinogen and its resistance to hydrolysis evoked
212 by snake venoms. *Comparative Biochemistry and Physiology Part B: Biochemistry and*
213 *Molecular Biology* 151: 428-432.
214
215 Weinstein, S. A., Smith, T. L., Kardong, K. V. 2009 *Reptile Venom Glands: Form, Function,*
216 *and Future*. In Handbook of Venoms and Toxins of Reptiles (ed S. P. Mackessy), pp. 65-91:
217 CRC Press.
218
219
220
221
222

PeerJ PrePrints

Figure captions

Figure 1. Photographs of an Egyptian saw-scaled viper (*Echis pyramidum*) that failed to hatch, most likely as a result of complications from a self-inflicted bite. Panel A was taken immediately after removal from the egg (panel E, showing slits from "pipping") and contains some substrate (vermiculite). The yolk evident in this panel suggests that death occurred prior to the absorption of the yolk mass. The specimen was preserved in 4% paraformaldehyde in a 52mm diameter Gosseline 100ml container (F) and packed in cotton wool for shipping and scanning (panel G). LJ = lower jaw.

Figure 2. Microtomography (µCT) scans show that the fangs (shaded red) are in the folded position and do not penetrate the body. A. whole specimen; B. frontal view; C. magnified view of the head/fang region from A; D. right view; E. left view, with digital dissection to 'remove' sections of the body for clarity.

PeerJ PrePrints

1

Figure 1

Photographs of an Egyptian saw-scaled viper (*Echis pyramidum*) that failed to hatch, most likely as a result of complications from a self-inflicted bite. Panel A was taken immediately after removal from the egg (panel E, showing slits from “pipping”) and contains some substrate (vermiculite). The yolk evident in this panel suggests that death occurred prior to the absorption of the yolk mass. The specimen was preserved in 4% paraformaldehyde in a 52mm diameter Gosseline 100ml container (F) and packed in cotton wool for shipping and scanning (panel G). LJ = lower jaw.

PeerJ PrePrints

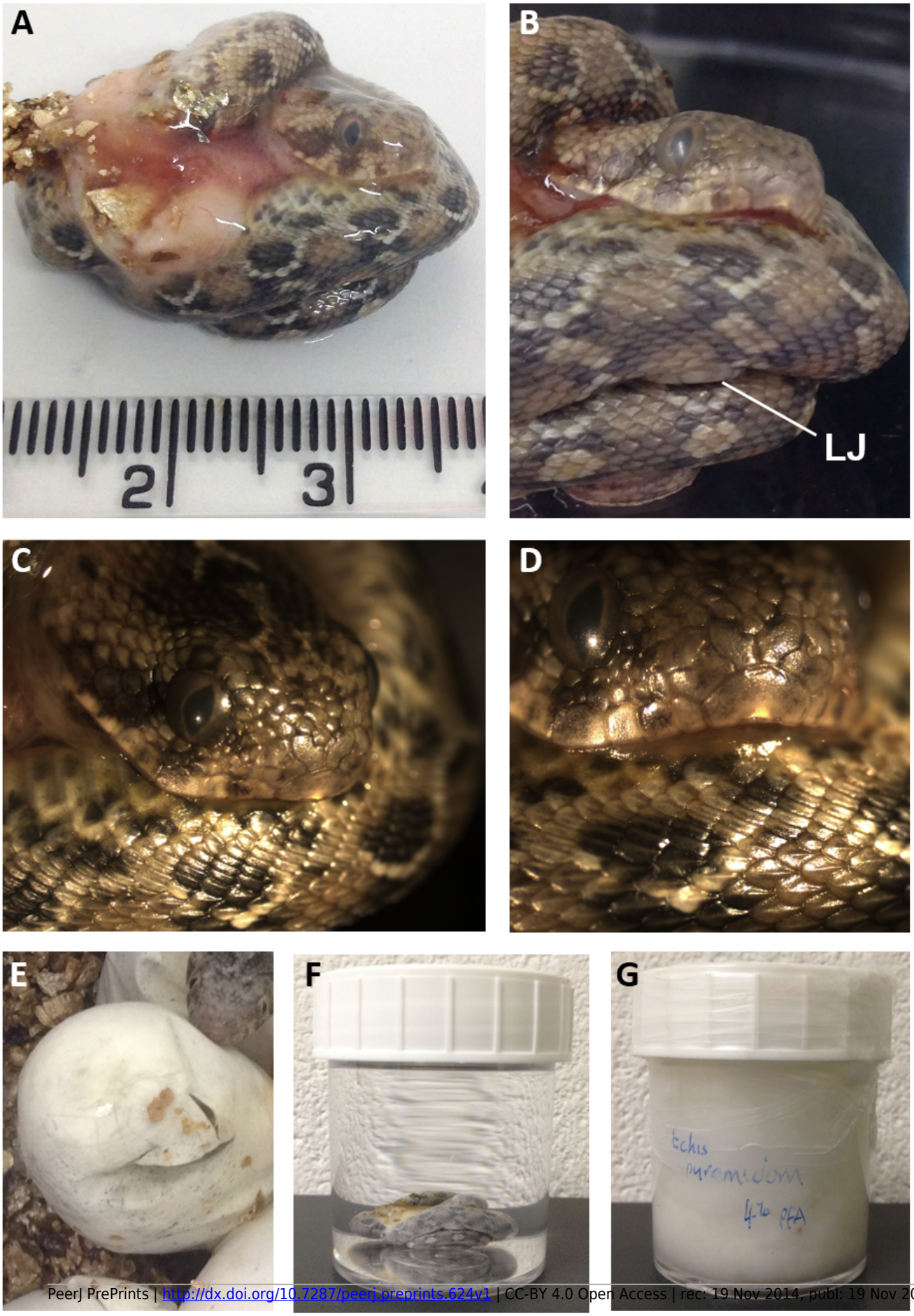

PeerJ PrePrints

PeerJ PrePrints | http://dx.doi.org/10.7287/peerj.preprints.624v1 | CC-BY 4.0 Open Access | rec: 19 Nov 2014, publ: 19 Nov 2014

2

Figure 2

Microtomography (μCT) scans show that the fangs (shaded red) are in the folded position and do not penetrate the body. A. whole specimen; B. frontal view; C. magnified view of the head/fang region from A; D. right view; E. left view, with digital dissection to 'remove' sections of the body for clarity.

PeerJ PrePrints

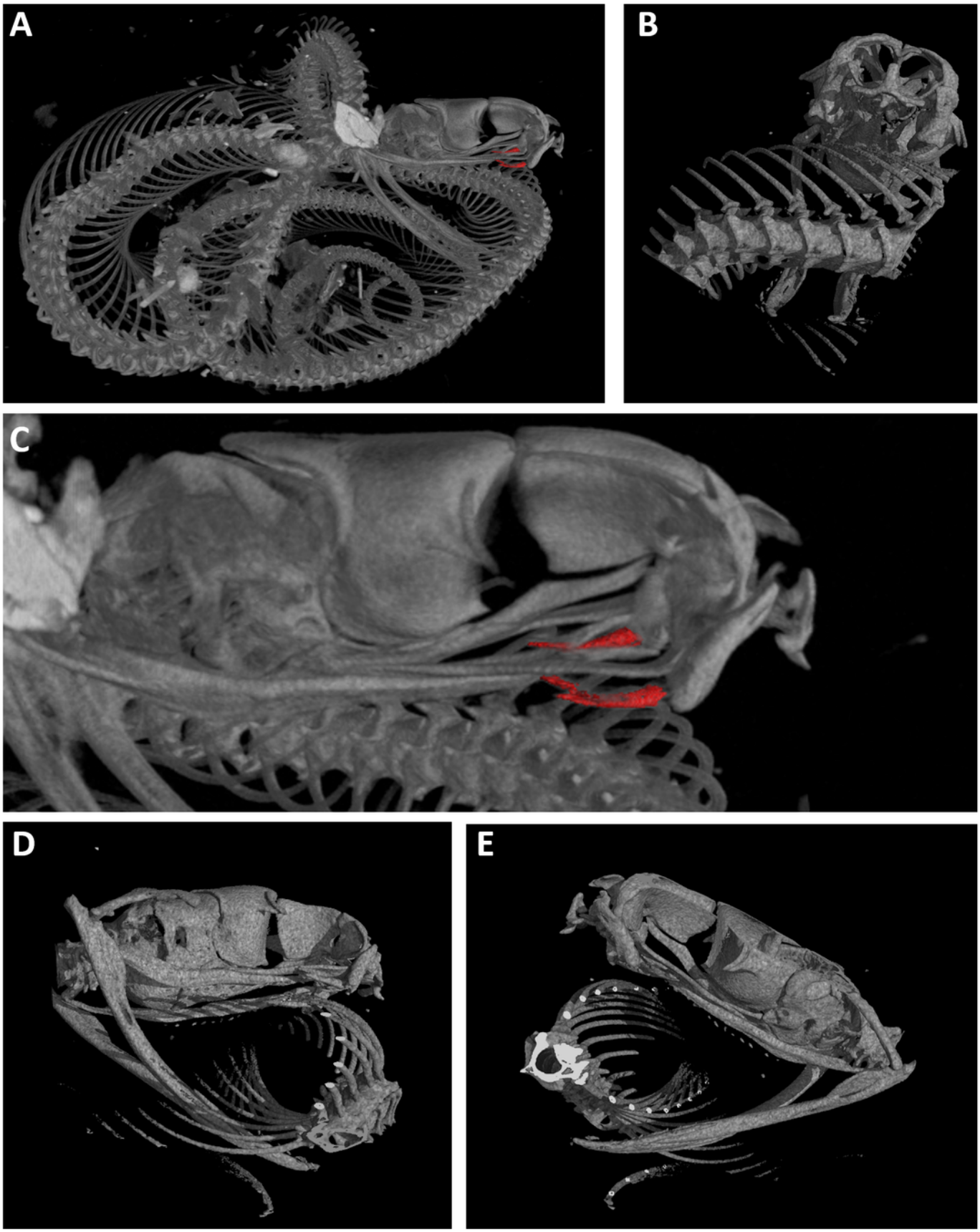

PeerJ PrePrints